The Liquid Argon Purity Demonstrator

M. Adamowski[a], B. Carls[a], E. Dvorak[b], A. Hahn[a], W. Jaskierny[a], C. Johnson[a], H. Jostlein[a], C. Kendziora[a], S. Lockwitz[a], B. Pahlka[a*], R. Plunkett[a], S. Pordes[a], B. Rebel[a], R. Schmitt[a], M. Stancari[a], T. Tope[a†], T. Yang[a]

[a]Fermi National Accelerator Laboratory, P.O. Box 500, Batavia, IL, 60510, USA

[b]South Dakota School of Mines & Technology, 501 East Saint Joseph Street, Rapid City, SD 57701

Contents

*Corresponding author: pahlka@fnal.gov (B. Pahlka)
†Corresponding author: tope@fnal.gov (T. Tope)

We report on measurements of the electron drift lifetime in the liquid argon and the associated measurements (contaminant concentrations and temperature) using the Liquid Argon Purity Demonstrator. We describe the apparatus, operational phases, and critical devices. The results show that long electron lifetimes can be achieved without initial cryostat evacuation, which is of particular interest in designing large liquid argon TPCs.

1. Introduction

1.1. TPC Introduction

Liquid argon (LAr) time projection chambers (TPCs) provide a robust and elegant method for measuring the properties of charged particle interactions by providing 3D event imaging with excellent spatial resolution. The ionization electrons created by the passage of charged particles through the liquid can be transported nearly undistorted by a uniform electric field over macroscopic distances. Imaging is typically facilitated by three sets of parallel wires, oriented with different directions and placed at the end of the drift path, continuously sensing and recording the signals induced by the drifting electrons. This technology relies on drifting ionization electrons from the site of energy deposition to readout wires up to two meters or more away without interaction with electronegative contaminants and has been employed successfully in both neutrino and dark matter experiments[REFS?]. This technology has experienced renewed and strengthened interest since having recently been chosen as the preferred technology for a future long-baseline neutrino oscillation experiment [1].

1.2. Previous Work

The ICARUS Collaboration has been leading a pioneering effort in the research and development of LAr TPC technology for the past 25 years. Their most recent TPC, the T600, is housed in a 760 ton cryostat. This cryostat is surrounded by insulating layers of Nomex honeycomb cells [2]. The volume of the cryostat was baked out under vacuum to 10^{-4} mbar before filling. Electron lifetimes greater than 6 ms were obtained with a contamination less than 0.1 parts per billion (ppb) water equivalent [3].

The Materials Test Stand (MTS) at the Fermi National Accelerator Laboratory (Fermilab) was developed to evaluate the effect of different materials on electron lifetime [4]. The system used a 250 L vacuum-insulated vessel that was evacuated before filling to a pressure of 10^{-6} Torr. The system purified commercial argon using filters similar to those described in Section 3.2maybe state them here. The MTS recorded electron lifetimes not in excess of 8 ms with a purity monitor similar to those detailed in Section 4.1.

Later at Fermilab, the ArgoNeuT project was the first LAr TPC in America to be placed in a neutrino beam [6]. Commissioned in 2009, it had an 550 L vacuum insulated cryostat that was evacuated before filling with LAr. The purification system also used similar filter materials to those discussed in Section 3.2, but was notably different in that it only purified reliquefied argon boil-off in the gaseous region of the cryostat. With this system, ArgoNeuT was able to obtain lifetimes of about 750 μs with typical drift fields.

The ARGONTUBE LArTPC of AEC-LHEP University of Bern was developed to investigate the ability to drift charge electrons? over distances of up to 5 m [7]. It uses used? still in operation? a vacuum insulated cryostat and was evacuated to 5×10^{-5} mbar before filling with

LAr. ARGONTUBE has been able to reach contamination levels down to 1 parts per million (ppm) and achieve lifetimes of 2 ms with a 240 V/cm drift field.

The conventional liquid argon vessels previously described are evacuated to remove water, oxygen, and nitrogen contaminants present in the ambient air prior to filling with liquid argon. However, as physics requirements dictate larger cryogenic vessels to hold bigger detectors, the mechanical strength required to resist the external pressure of evacuation becomes prohibitively costly.

1.3. The Liquid Argon Purity Demonstator

The Liquid Argon Purity Demonstrator (LAPD) located at Fermilab is designed to achieve, with a straightforward procedure, the ultra high purity required by LArTPCs in a vessel that cannot be evacuated. The purification of the volume proceeded in three stages to obtain electron lifetimes on the order of several milliseconds. The system relies heavily on the experience from the MTS at Fermilab [4] in its design and operation plan. Prior to filling with liquid argon, the ambient air is removed by purging the tank with argon gas. It has been shown that the concentration of oxygen in a vessel purged with gaseous argon can be reduced to 100 ppm after 2.6 volume exchanges [5]. After the initial volume exchange, an optional step was to heat the walls of the cryostat to dry the surfaces of the vessel and monitors in the gas. Once the water and oxygen concentrations are at the level of ppm, the gas is subsequently circulated through filter vessels to further reduce these contaminants. Finally, liquid argon is then introduced into the vessel after a concentration of impurities less than 1 parts-per-million (ppm) is achieved. The liquid is continuously circulated through the filter vessels in order to achieve concentrations of water and oxygen on the order of 0.1 parts-per-billion (ppb). A photograph of the LAPD is shown in Figure 1.

In addition to the primary goal of the LAPD, several other parameters were evaluated. First, we monitored temperature gradients in the bulk liquid and concentrations of water and oxygen in order to check our models for the behavior of the liquid. Second, we studied the number of liquid argon volume exchanges necessary to achieve drift distances on the scale of 2.5 meters. Third, the filter capacity as a function of flow rate was closely monitored and its performance evaluated. Finally, after achieving the required electron drift lifetimes, the LAPD was emptied and a TPC of 2 m drift distance was placed in the volume. High LAr purity was achieved with the TPC in the tank. The details of the TPC and its performance will be discussed in a separate paper.

This document is outlined as follows. The LAPD vessel is described in Section 2. The cryogenics, including larger filters and upgraded cryogenic valves from the MTS, are detailed in Section 3. Section 4 discusses the instrumentation to monitor the LAr including the purity monitors, gas analyzers, and temperature-monitoring devices. Finally, Sections 5 and 6 conclude with the results and a brief discussion.

2. The Tank

The LAPD cryostat is an industrial low pressure storage tank. The tank has a flat bottom, cylindrical sides, and a dished head. The tank diameter is 10 feet and the cylindrical walls have a 10-foot height. The tank is fabricated from 3/16 inch-thick SA-240 stainless steel. The internal and external (vacuum) maximum allowable working pressures are 3 psig and 0.2 psig, respectively. Eight perimeter anchors tie the tank bottom to the ground to prevent tank uplift. The tank volume is 6506 gallons of which 5603 gallons is liquid (32.6 tons) with a corresponding liquid depth of 2.9 m. Fabrication followed The American Petroleum Institute Standard 620 Appendix Q as closely as possible. The tank welds were fully radiographed. The tank is located

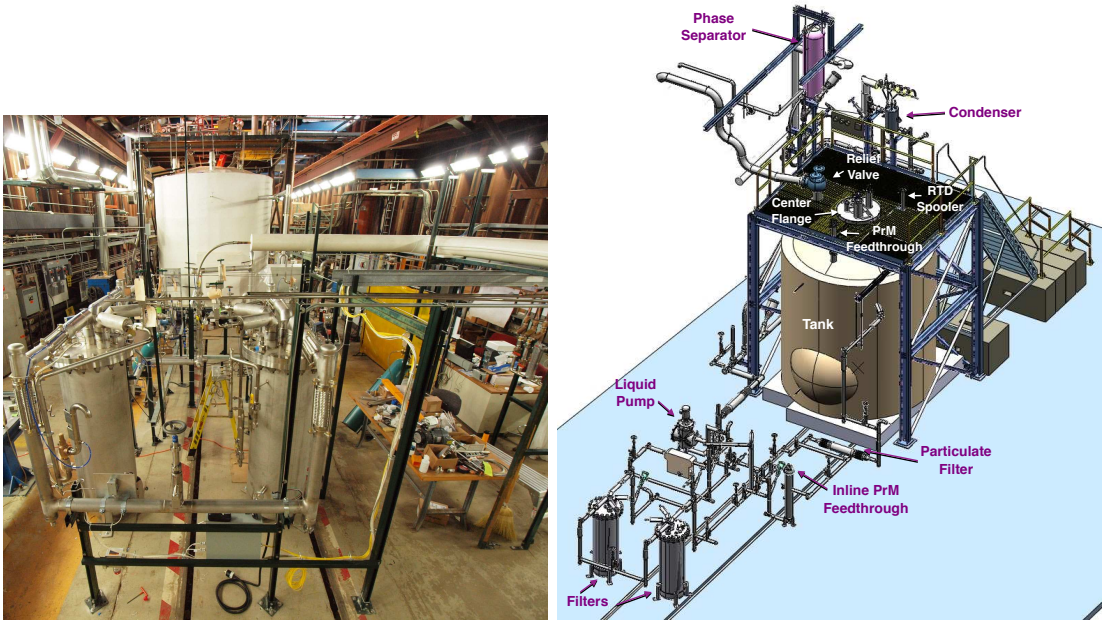

Figure 1. A photograph of the Liquid Argon Purity Demonstration (LAPD) at Fermilab (left) and 3D model of the system (right).

inside the Proton Center 4 building at Fermilab. Figure 2 shows a picture of the LAPD tank.

The head of the tank is populated with four ConFlat flanges and a 30 inch diameter center flange sealed with an indium wire. Metallic seals are used to prevent the diffusion of contamination that would occur through non-metallic seals. The center flange allows for tank entry using an extension ladder. Five ConFlat flanges populate the center flange, each of which sit atop stainless steel tube risers such that the ConFlats remain at room temperature when the cryostat is cold. Figure 3 shows the top of the tank layout. At ground level a 30 inch diameter welded manhole is available and intended to make access easier for extended work inside the tank.

The tank sides and top are insulated with 10 inches of fiberglass which is covered by an outer layer of 3/4 inch-thick foam. The foam is covered with glass cloth and a mastic which provides a vapor barrier. The tank sits on an insulating structural foam base also sealed with a mastic vapor barrier. The tank heat leak is estimated as 2103 W. The foam base sits atop two rail cars and cribbing. Natural air flow under the rail cars and cribbing eliminates the need for foundation heaters.

The tank was cleaned with deionized water and detergent then dried with lint free rags by the tank fabricator prior to shipment to Fermilab. After installation of all components at Fermilab the tank was vacuumed with a HEPA filter equipped vacuum. After vacuum cleaning, all walls were wiped with deionized water and lint free rags. Stubborn residue was spot removed with alcohol and lint free rags.

Figure 2. LAPD tank sitting on an insulating structural foam base in PC4. Insulating foam was added to the sides and head later.

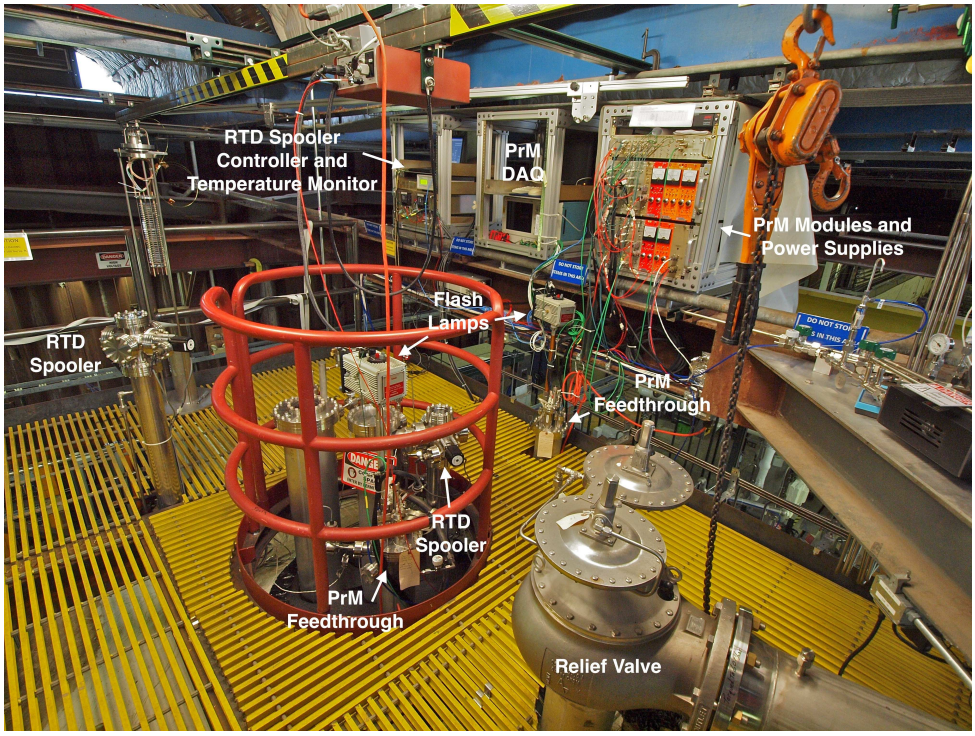

Figure 3. A photograph of the platform on top of the tank. The purity monitor feedthroughs, RTD spoolers, and the control systems are shown.

3. The Cryogenics

3.1. Phase Separator and Condenser

The argon vapor generated by ambient heat input is condensed using liquid nitrogen. A 4000 gallon trailer supplies liquid nitrogen through foam insulated 1 inch Type K copper piping. A phase separator operation at 15 psig near the LAPD cryostat vents nitrogen vapor generated in the nitrogen transfer line so that the condenser is supplied with single phase liquid nitrogen. A control valve feeding the phase separator maintains a constant liquid level in the phase separator. The condenser consists of an argon volume containing three differently sized coils of tubing through which liquid nitrogen flows. The coiled nitrogen tubing is seamless and all nitrogen connections and welds are outside the condenser to mitigate any nitrogen leak into the LAPD cryostat. Argon vapor generated by ambient heat input into the LAPD cryostat is condensed by the liquid nitrogen flowing through the coils.

By default, the condensed liquid argon returns to the liquid recirculation pump suction and then goes through the filters during liquid recirculation. This is important since the water outgassing from tank wall above the liquid is mixed with the argon vapor and needs to be removed in order to maintain good LAr purity. When the pump is off, the condensed liquid argon returns directly to the tank. A control valve feeds the condenser and adjusts the flow to maintain a constant vapor pressure in the ullage. Solenoid valves choose which coil or which combinations of coils receives liquid nitrogen. The calculated cooling capacity of the condenser is 8400 W (reference). The coils operate at near ambient pressure due to the pressure drop across the inlet control valve. They therefore must be covered in a thin layer of argon ice to achieve the required temperature gradient. The vaporized nitrogen is vented outside the enclosure and not recovered. Figure 4 showers the sketch of the condenser designed and Figure 5 shows a photo of the phase separator and condenser in PC4.

3.2. Filters

The purification system contains two filters which have identically sized filtration beds of 77 liters. The first filter that the process stream enters contains a 4A molecular sieve supplied by Sigma Aldrich (reference). The 4A molecular sieve primarily removes water contamination but can also remove small mounts of nitrogen and oxygen. The second filter contains BASF CU-0226 S, a highly dispersed copper oxide impregnated on a high surface area alumina to remove oxygen(reference). The oxygen filter will also remove water such that removing water from the process before it enters the oxygen filter maximizes the oxygen filter capacity needs rework. The filters are insulated with vacuum jackets and aluminum radiation shields. Metallic radiation shields were chosen because the filter regeneration temperatures would damage traditional aluminized mylar insulation. Piping supplying the filter regeneration gas is insulated both inside the filter vacuum insulation space and outside the filter with Pyrogel XT which is an aerogel based insulation (reference) which can withstand temperatures up to 1200 F. Figure 6 shows the 3D model of the filter vessel.

The filters are regenerated in place using heated gas. The molecular sieve is regenerated using a flow of argon gas heated to 200 C. The argon gas is supplied by commercial 180 liter liquid argon dewars. The oxygen filter is also heated to 200 C using argon gas. Once at 200 C, a small flow of hydrogen is mixed into the primary argon flow. The hydrogen combines with oxygen captured by the filter and creates water. The hydrogen fraction does not exceed 2.5% of the heated gas mixture. The regeneration reaction is exothermic such that too much hydrogen causes excess temperatures that damage the filter by sintering the copper and greatly reducing the available filter surface area. During the heated gas regeneration, five filter bed temperature sensors monitor the filter material temperature and the water content of the regeneration exhaust

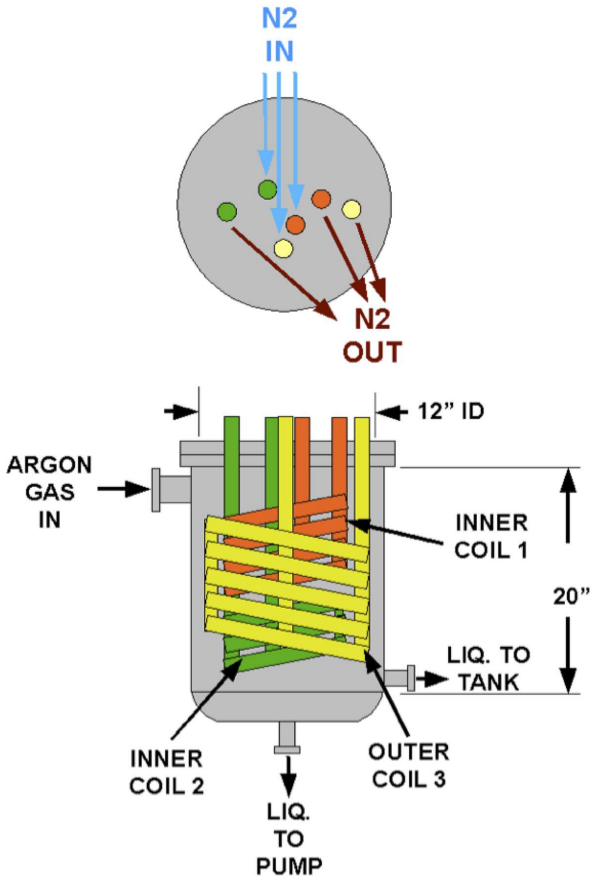

Figure 4. A sketch of the LAPD condenser which shows the three coils of tubing for liquid nitrogen, the inlet for gaseous argon and two outlets for liquefied argon.

Figure 5. A photograph of the LAPD phase separator and condenser. The argon vapor path to the condenser and the two liquefied argon return paths are shown.

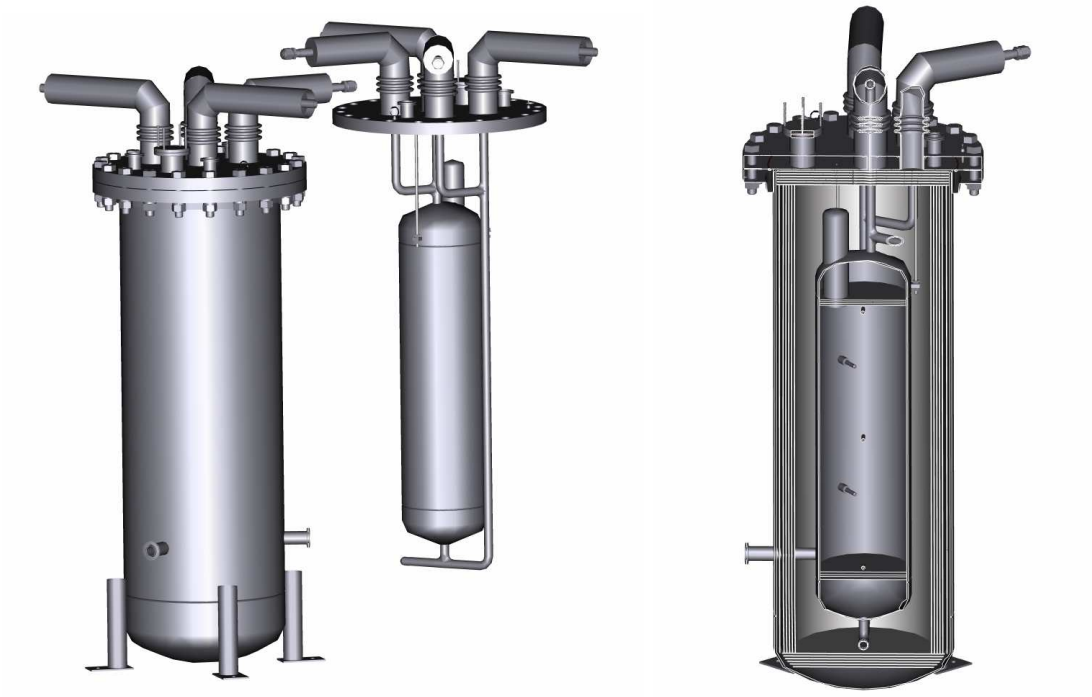

Figure 6. 3D model of the filter vessel. The evacuation vessel and the canister holding the filter material are shown on the left. The cross section of the vessel is shown on the right.

gas is measured. Both filters are evacuated using turbomolecular vacuum pumps while they cool to remove remaining trace amounts of water.

At the filtered liquid return to the tank, a particulate filter with an effective filtration of 10 microns protects the tank from any debris in the piping. The filter consists of a commercial stainless steel sintered metal cylinder mounted in a custom cryogenic housing and vacuum jacket. Flanges on the argon piping along with flanges and edge welded bellows on the vacuum jacket allow removal of the particulate filter. Liquid argon flows to the interior of the sintered metal cylinder and then outward through the walls of the sintered metal cylinder which provide filtration.

3.3. Piping and Valves

The Schedule 10 stainless steel purification piping that supplies argon to the filters is vacuum jacketed. The inner line containing argon is 1 inch in diameter with a 3 inch diameter vacuum jacket, except at the pump suction where the inner line is 2 inches in diameter with a 5 inch diameter vacuum jacket. During the fabrication process, all piping was washed with deionized water and detergent to remove oil and grease. Lint free rags wetted with alcohol were pulled through the pipes until no contamination was visible on the rag. All valves associated with the argon purification piping utilize a metal seal with respect to ambient air either through a bellows or a diaphragm to prevent the diffusion of oxygen and water contamination. The exhaust side of relief valves is continuously purged with argon gas such that diffusion of oxygen and water from ambient air across the o-ring seal is prevented. Where possible, ConFlat flanges with copper seals are used on both cryogenic and room temperature argon piping. Pipe flanges in the system are sealed using spiral wound graphite gaskets (reference). Smaller connections are made with VCR fittings with stainless steel gaskets.

3.4. Recirculation Pump

The liquid argon pump is a Barber-Nichols BNCP-32B-000 long shaft argon pump. It is a partial emission centrifugal pump with a magnetic drive to isolate the pump and liquid argon from the electric motor. The pump shaft with the impeller, inducer and driven section of the magnetic coupling have their own bearings which are lubricated by the liquid argon at the impeller end and are non-lubricated at the coupling end. The motor is controlled by a variable frequency drive (VFD) which allows adjustment of the pump speed to produce any desired head and flow within the available power range of the motor. A photograph of the liquid pump is shown as Figure 7.

The liquid argon flow rate is measured at the pump discharge by an Emerson Process Management Micro Motion Coriolis flow meter. This flow meter is appropriate for ultra high purity liquid argon because, from the perspective of the liquid argon, it only consists of stainless steel pipe and flanges. The inertial effects of the fluid flow through the flow meter pipes is directly proportional to the mass flow of the liquid. The mass flow rate is computed by measuring the difference in the phase vibration between one end of the flow pipe and the other. The flow curve of the liquid argon pump with respect to mass flow and pressure is quite flat, such that pump speed and differential pressure are not good indicators of the mass flow rate. Thus the liquid argon flowmeter is essential instrumentation if the rate of filtration is to be known.

3.5. Control System

The LAPD cryogenic system is controlled by a Siemens Programmable Logic Controller (PLC). The PLC reads out the pressure, liquid level, temperature, gas analyzer instrumentation, and electron lifetime measured by purity monitors. Human machine interface controls are provided through GEFANUC's iFIX software running on a Windows PC, which is connected to the

Figure 7. A picture of the liquid pump.

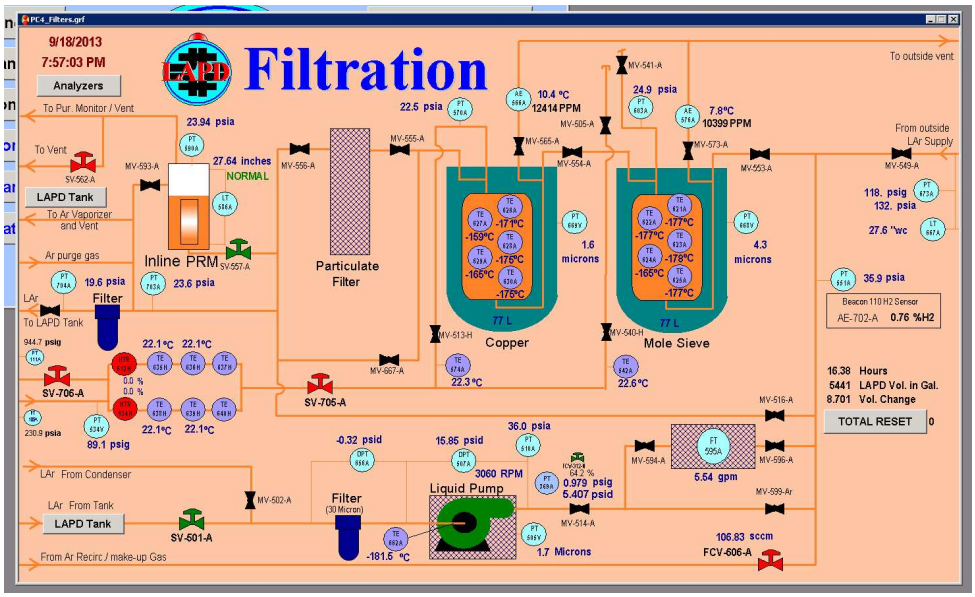

Figure 8. An example of iFIX graphical user interface for the LAPD controls.

PLC through local ethernet. The iFIX software allows entry of temperature and pressure set points and other operational parameters, handles alarming and remote operator controls such as opening and closing valves, displays real-time instrument values, and archives instrument values for historical viewing. An example of the iFIX graphical user interface used in the LAPD is shown in Figure 8.

4. Tank Instrumentation

In this section we describe the instruments located inside the tank for the purity and temperature measurements including the purity monitors, the gas analyzers, and the RTD spoolers. Figure 9 shows the locations of purity monitors and RTD spoolers inside the tank.

4.1. Purity Monitors

4.1.1. Hardware

A dedicated monitoring device, called a purity monitor, is used to determine the purity of the liquid Argon. The purity monitor is a double-gridded ion chamber immersed in the liquid Argon volume based on the design described in Reference [9]. It consists of four parallel, circular electrodes: a disk supporting a photocathode, two open wire grids (anode grid and cathode grid) and an anode disk. The anode disk and photocathode support disk are made of stainless steel; the two grid support rings are made of G-10 circuit board material with the grid wires soldered to the copper clad surface. The region in between the anode grid and cathode grid contains a series of field-shaping stainless steel rings. The two grids, each with a single set of parallel wires, are made of electro-formed gold-sheathed tungsten (AuW) with a 2.0 mm wire spacing, 25 μm wire diameter and 98.8% geometrical transparency.

The cathode grid is at ground potential. The cathode, anode grid, and anode are electrically accessible via modified vacuum grade high voltage feed-throughs. The anode grid and the field-shaping rings are connected to the cathode grid by an internal high-value resistor chain (50 MΩ

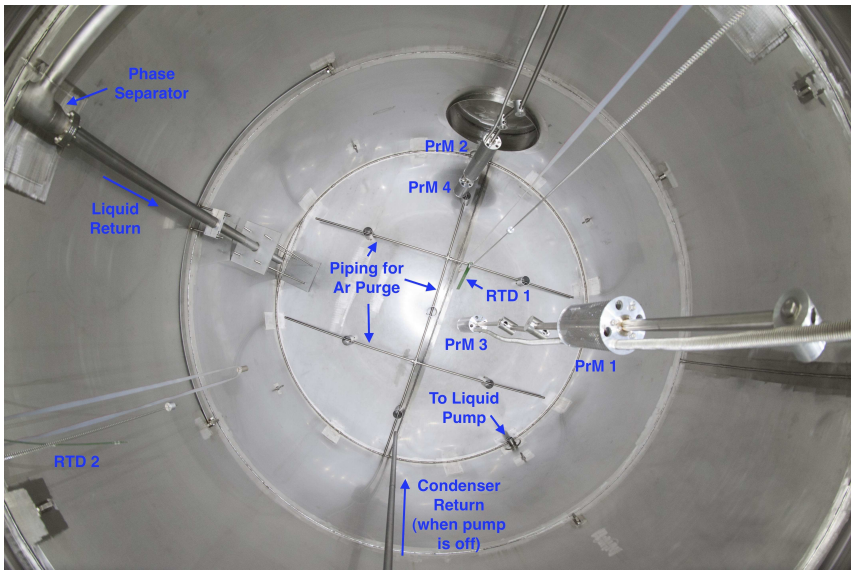

Figure 9. A photograph of the interior of the tank. The purity monitors, RTD spoolers and piping are shown.

each) to ensure the uniformity of the electric fields in the drift regions. The field ratios typically satisfy

$$E_{Anode\ Grid-Anode} > 2E_{Anode\ Grid-Cathode\ Grid} > 4E_{Cathode\ Grid-Cathode} \quad (1)$$

to ensure maximum transparency [10].

The photocathode[3] is a $1'' \times 3'' \times 1/32''$ aluminum slide, coated with 50 Å of titanium and 1000 Å of gold and attached to the cathode disk. A xenon flash lamp[4] is used as the light source. The UV output of the lamp has a wide spectrum above approximately 225 nm. An inductive pickup coil on the power leads of the lamp provides a trigger signal when the lamp flashes. Light is directed via three quartz optical fibers[5] (only one fiber is needed the other two are for redundancy) to the photocathode. The fibers have a 0.6 mm core diameter and 25.4 degrees of full acceptance cone. The attenuation is 0.95 dB/m at $\lambda = 200$ nm. The electrons liberated from the photocathode drift towards the cathode grid and induce a current on the cathode. After crossing the cathode grid, the electrons drift between the two grids. During this time essentially no current is induced on the cathode or anode due to the shielding effect of the grids. After crossing the anode grid, the electrons induce a current on the anode. The signals induced on the cathode and anode are fed into two charge amplifiers in a purity monitor electronics module. The charge amplifiers have a 5 pF integration capacitor with a 22 MΩ resistor in parallel with the capacitor. The signal and high voltage are carried on the same cable and decoupled inside the purity monitor electronics module. Figure 10 shows a schematic of the liquid argon purity monitor.

The LAPD system employs five purity monitor units at different locations. Each purity monitor is contained in a stainless steel, perforated Faraday cage to isolate the system from the

[3]Made by Platypus Technologies, LLC, Madison, WI
[4]Made by Newport, Stratford, CT
[5]Made by Polymicro Technologies, Phoenix, AZ

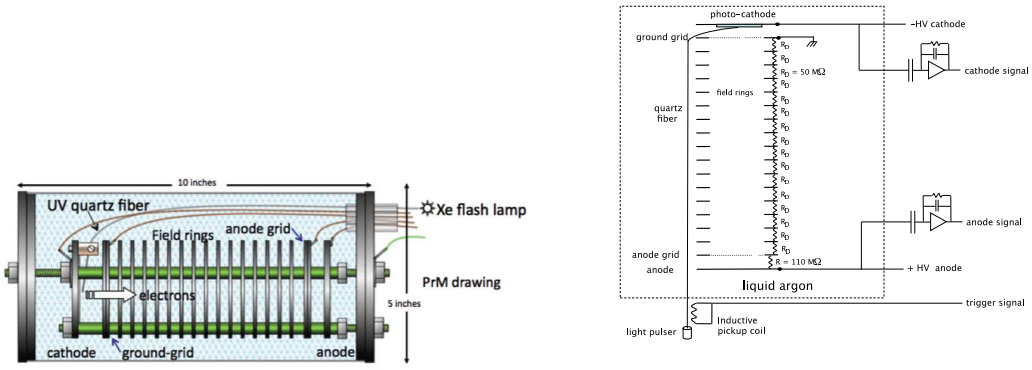

Figure 10. Drawing and schematic of Liquid Argon Purity Monitor.

outside electrostatic interference. There are two types of purity monitors with different lengths and different numbers of field-shaping rings: three long purity monitors that are 55 cm and two short purity monitors that are 24 cm. T/F? necessary? The longer electron drift time in the long purity monitor ensures a more accurate lifetime measurement. An assembly of one long purity monitor and one short purity monitor is located vertically along the central axis of the tank. Another identical assembly is located at a distance of 1.1 m away from the center of the tank. Figure 11 shows a photograph of the assembly located near the tank periphery. One long purity monitor (referred to as the inline purity monitor) is located in the circulation pipe to measure the liquid Argon purity before the liquid enters the tank. Three flash lamps are used for the two purity monitor assembles and the inline purity monitor. Table 1 shows the geometrical characteristics and voltage settings of the purity monitors installed in the tank.

4.1.2. Data Acquisition

A Visual Basic program running on a Tektronix[6] digital storage oscilloscope (5054 TDS) is used for control and data acquisition for the purity monitor system. The program controls operations through the Automation Module, which controls the high voltage power to the purity monitor and the flash lamp operation. Measurements of the electron lifetime are taken several times a day. Each measurement of the drift-lifetime takes about a minute. The flash lamp and the high voltage to the purity monitors are only powered during this time to protect the flash lamp, minimize degradation of the quartz fiber and reduce dust/particle accumulation on the purity monitor. The automation module will switch off both the flash lamp power supply and high voltage to the purity monitor if the lamp has been flashing for more than 140 seconds.

An 8-channel analog MUX is used to select purity monitor signal readouts. Each channel of the MUX has four inputs, three of which read the cathode and anode signals from one purity monitor after the amplifiers and the trigger signal from the inductive pickup coil. The program communicates with the MUX through the 5054 parallel port and sends a signal to the MUX to select one of the five purity monitors. The MUX then sends a signal to the automation module to switch on the high voltage power to the selected purity monitor and flash lamp. The MUX also sends the relevant trigger, cathode, and anode signals to the scope.

[6]Tektronix, Inc., Beaverton, OR

Figure 11. One assembly of one long purity monitor and one short purity monitor inside LAPD.

Table 1
Geometrical characteristics and voltage settings of the purity monitor.

	Long monitor	Short monitor
Cathode, Anode disk, grid diameter	8 cm	
Cathode-Anode total drift distance	50 cm	19 cm
Cathode grid to Anode grid distance	47 cm	16 cm
Cathode-Cathode Grid gap	1.8 cm	
Anode Grid-Anode gap	0.79 cm	
Number of field-shaping rings	45	15
Number of resistors	46	16
Anode disk/Cathode disk thickness	0.23 cm	
Anode grid/Cathode grid thickness	0.24 cm	
Field-shaping ring thickness	0.23 cm	
Gap between rings	0.79 cm	
Nominal Cathode Voltage	-100 V	-100 V
Nominal Anode Voltage	5 kV	2 kV
$V_{Anode\ Grid}/V_{Anode}$	0.948	0.865
Nominal $E_{Cathode\ Grid-Cathode}$	56 V/cm	56 V/cm
Nominal $E_{Cathode\ Grid-Anode\ Grid}$	101 V/cm	108 V/cm
Nominal $E_{Anode\ Grid-Anode}$	329 V/cm	342 V/cm

The program in the TDS 5054 oscilloscope digitizes the signals after the high voltages stabilize and calculates the electron lifetime (τ) based on the ratio of anode and cathode signals ($Q_{anode}/Q_{cathode}$) and the electron drift time (t) - the time between the cathode and anode signals - using the relation [9]

$$Q_{anode}/Q_{cathode} = e^{-t/\tau}. \quad (2)$$

The program turns on each purity monitor and reads out the signals one by one. Figure 12 shows the block diagram of LAPD purity monitor system.

During the initial operation, we observed the presence of large noise components generated by the flash lamp particularly in the cathode and anode signals. The noise affects the waveforms and makes it difficult to measure the amplitudes of real signals. We modified the automation module and the DAQ program to measure the noise before we measure the real signals. The program first sends out a signal to the MUX to ask the automation module to switch on the flash lamp power supply without switching on the high voltage power to the purity monitor. The scope stores the waveforms, which provide an estimate of the noise. Then the program sends out another signal to turn on the high voltage power to the purity monitor in addition to the flash lamp. The noise is then subtracted from the measured waveforms to get the real cathode and anode signals.

For the second run of LAPD, the purity monitor DAQ system, previously consisting of a Tektronix oscilloscope, was replaced by an off-the-shelf PC equipped with a PCI digitizer card. The digitizer card is a 12-bit AlazarTech ATS310 card capable of sampling at 20 MHz. The new DAQ system performed as well as the oscilloscope and was procured at a cheaper cost. The original Visual Basic purity monitor DAQ program from the first run was modified to run with the digitizer utilizing the development kit for the ATS310.

For each acquisition, the digitizer recorded and averaged at least ten samples for each of the

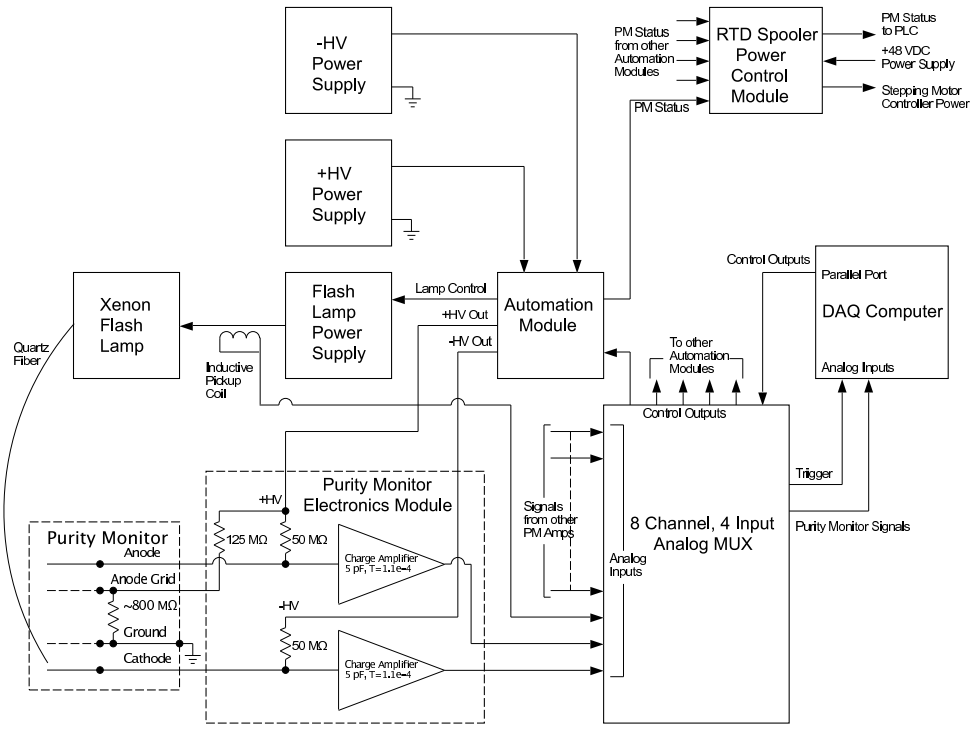

Figure 12. Block diagram of LAPD purity monitor system.

traces needed. For the long purity monitors, the sampling rate used was 2 MHz and for the short purity monitors, 5 MHz. The range of voltages used used for both long and short purity monitors was ±50 mV. A plot of the averaged signal traces produced from the digitizer card, before and after noise subtraction, is shown in Figure 13.

An additional source of electrical noise that affected the operation of the purity monitor DAQ was found to be the RTD spooler stepping motor controllers. These controllers have a DC to DC switching converter that provides the holding current to the stepper motors used in the RTD spooler system. The most effective way to deal with this noise source was to remove the 48 Volt DC bulk power to the stepping motor controllers whenever the purity monitor DAQ was running. After the purity monitors were turned off by the DAQ, the 48 Volt DC power was restored to the stepping motor controllers and a reset signal was given to the controllers so that they would reindex back to the zero starting point for their data collection.

4.1.3. Fiber Quality checks

We use three single-mode quartz optical fibers to illuminate the each purity monitor photocathode. The separation distance of each fiber end with respect to the mercury lamp bulb is about 1 mm for three of the fibers and about 0.75 mm for a fourth. The separation distance of each fiber with respect to the photodiode collar has a range of 0.216 inches to 0.239 inches, measured with a digital caliper. This relative offset is corrected for in the response and provides about 1% relative change.

The fibers underwent a series of tests to measure the stability and light output linearity as a function of input light intensity. The tests were performed using a simple analog photodiode

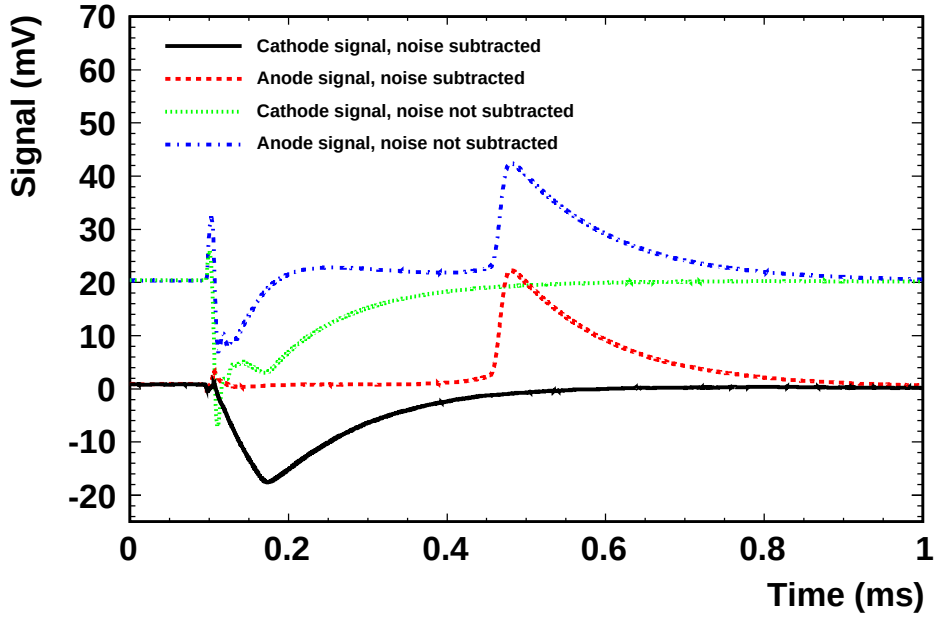

Figure 13. A screenshot of anode and cathode signals before and after noise removal from the digitizer.

read out by an oscilloscope. Fibers were positioned with one end in close proximity to the light source and the other end in close proximity to the photodiode. Measurements of the photodiode response for a single fiber were taken for several values of relative input intensity as reported on the mecury lamp light source with results suggesting a linear response. The variation in the photodiode response was measured by recording ten consecutive measurements for each fiber and showed maximum relative deviations of 5%. Finally, for each fiber, the photodiode response was measured with the light source placed in a vertical configuration and a horizontal configuration and showed no changes. The fiber cleaves were inspected and showed no anomalous behavior. However, three fibers indicating a nominal response had a small, sharp edge sticking out. The fiber with the highest response had the opposite, much like a small "chip" out of the edge. These studies suggest that the employed fibers were suitable for accurately delivering the light from the lamp to the photocathode. There are plots of each of these studies that I chose not to include.

4.1.4. Systematics

There are several systematic effects which need to be accounted for to make a reliable measurement of argon purity. The lifetime relies on measurements of V_{anode} and $V_{cathode}$, which in turn depend on amplification of induced currents on the anode and cathode. The potential exists for differences in amplification between the anode and cathode signal voltages to have an impact on the lifetime. We model the amplification as $V_{anode} = g^{\alpha}Q_{anode}$ and $V_{cathode} = g^{\beta}Q_{cathode}$, where g^{α} and g^{β} are constants. If the two amplifiers used for the anode and cathode signals are switched, the amplification becomes $V'_{anode} = g^{\beta}Q_{anode}$ and $V'_{cathode} = g^{\alpha}Q_{cathode}$. The primes indicate measurements taken with the amplifiers for the anode and cathode swapped.

The lifetime and attenuation calculations can then be calibrated by making measurements of V_{anode}, V'_{anode}, $V_{cathode}$, and $V'_{cathode}$ using

$$\frac{g^{\alpha}}{g^{\beta}} = \sqrt{\frac{V_{anode}/V_{cathode}}{V'_{anode}/V'_{cathode}}}. \tag{3}$$

During a span of several days with relative constant argon purity, measurements were taken with the amplifiers swapped to measure the ratio g^{α}/g^{β}. With the measurements taken, a correction to the lifetimes was applied using

$$\tau = \frac{t}{\ln((V_{cathode}/V_{anode}) \times (g^{\alpha}/g^{\beta}))}. \tag{4}$$

Another systematic examined is the effect of the values of the high voltages applied to the cathode and anode. To examine this effect, the high voltages applied to the anode and cathode were varied and many measurements were taken during a span of a few hours with relative constant purity. A short purity monitor was run with high voltages on the anode at 2 kV, 3 kV, 4 kV, and 5 kV. We need a conclusion with some percentages along with the 1.028 correction.

4.2. Gas Analyzers

4.2.1. Oxygen, Water and Nitrogen Monitors

LAPD has an extensive gas analysis system to monitor and diagnose the processes that take the tank from atmospheric air to ultra pure liquid argon. The system consists of seven commercial gas analyzers. Four of these analyzers measure the oxygen concentration and together they span the range from 0.1 ppb to 5000 ppm. These four oxygen analyzers are augmented by two 0.1-25% oxygen sensors which monitor the purge of the tank from air and are described in Sec. 4.2.2. Two of these seven gas analyzers measure the water concentration and these span the range from 0.2 ppb to 20 ppm. Dew point meters installed in series with these water analyzers extend the measurement range from 20 ppm up to ambient dew points as high as 20,000 ppm water. A nitrogen analyzer completes the array of seven gas analyzers with a range that spans 0.1 to 100 ppm.

The gas analyzers are fed by a local switchyard of 56 diaphragm valves. These valves direct the gas flow from five primary locations in the system to the seven gas analyzers. In addition to the five primary locations, argon and nitrogen gas from utility sources are available to supply analyzers when measurement from a system location is not required. A primary location or utility gas can feed anywhere between none and all of the gas analyzers. The primary measurement locations are the liquid argon tank (secondary location selection between vapor and liquid phases), pump discharge, molecular sieve filter output, oxygen filter output, and the liquid argon fill connection. An oil free vacuum pump is also part of the switchyard and can evacuate the tubing that connects the measurement locations and the gas analyzers. Evacuation of the sample lines when switching sample locations greatly reduces the time required to reach equilibrium when the measured contamination is at the parts per billion concentration. A high purity metal bellows pump boosts the sample pressure from the 2 psig operating pressure of the liquid argon tank to the 15-20 psig inlet pressure required by the gas analyzers. A photograph of the gas distribution switchyard is shown as Figure 14.

Filter output sampling allows determination of filter performance and capacity. Sampling the liquid argon fill connection is critical to ensure that the liquid argon supply is within specification. A trailer of liquid argon was rejected because it was so far out of specification it would have required an impractical number of filter regenerations to process. Without this extensive gas analyzer system it would be very difficult to successfully take the tank from ambient air to ultra pure liquid argon.

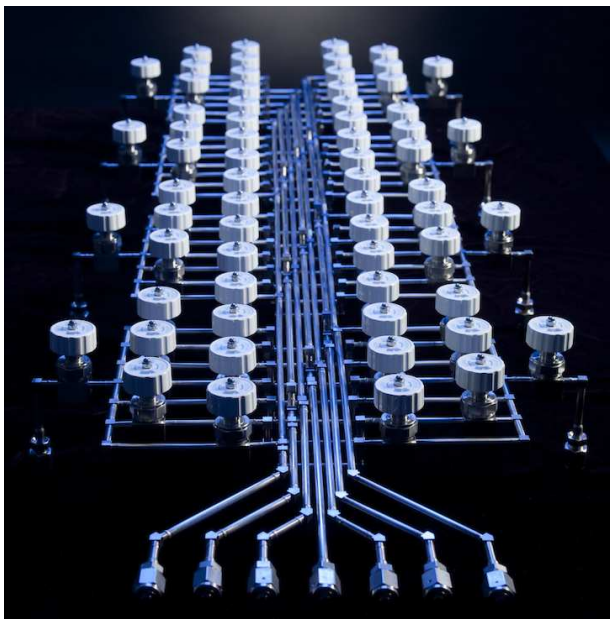

Figure 14. Gas distribution switchyard - liquid argon gas sampling master distribution panel.

4.2.2. Oxygen sniffers

We deployed 14 industrial type oxygen sensors (Citicell model 2FO), configured in two strings of 7 each with one placed near the tank wall and the other near the tank center, to measure the oxygen concentration during the initial gaseous argon purge. Their vertical spacing is about 30 inches spanning the height of the tank. The sensors are inside glass "jam jars" with plastic coated lids. The sample tubes are 0.063 inch diameter capillaries, and run continuously from the intake point through a CF flange to the jars. All capillaries are the same length, with the excess length coiled up above the feed-through flange, to assure matched time response. The jars are mounted on feed-through flanges.

4.3. RTD Spoolers

This section needs to be shortened and wordsmithed. We installed two sets of three resistive thermal devices (RTDs) on translators (also called "Spoolers") which are deployed to measure thermal gradients in the tank at all stages of operation (gas purge, liquid filling, partially filled tank and full tank). When there is liquid in the tank, the RTDs measure the temperature of both the liquid and the gas in the ullage. Spooler #1 is installed near the center of the tank and Spooler #2 is installed 1.0 m radially outward from the center.

The motivation for the Spooler is to help verify finite element analysis (FEA) calculations [11] that are used to model LAr mass flow in the cryostat. These calculations are important to understand if potential current eddies might occur under certain circumstances. These eddies might concentrate impurities or even positive space charge in a TPC detector environment, leading to difficulty with making track measurements that pass through these regions. Gas flow in the ullage which can mix impurities into the liquid are also calculated by FEA [**?**]. At this point, temperature gradients are the only experimental way we have to verify the calculations. LARTPC-doc-635-v4 has a prediction for temperature as a function of position. It may be good

to overlay the prediction on Fig 17.

Each Spooler consists of a single circuit board, 50 cm long with resistive thermal devices (RTDs) mounted at 22.9 cm intervals for a total of 3 RTDs per circuit board as can be seen in Figure 15. The circuit board is suspended at one end of a chain with a counter-weight at the other end of the chain to prevent movement during an electrical outage. The central chain is 3 m long and the radial chain is 2.5 m long – the difference arises from the shape of the sloping top of the tank. The chains engage a 15.13 cm circumference gear that is driven externally, through a ferromagnetic seal, by an Automation Direct STP-MTRH-23079 stepper motor. The housing around the gear also includes electrical limit switches to stop the motor when the chain limits are reached. The stepper motor is controlled by an Automation Direct STP-DRV-4850 stepper drive. During a typical Spooler run, the circuit board translates vertically through the tank with stops at predefined locations to take temperature measurements.

A ribbon cable connects one end of the circuit board to a feed-through at the top of the tank, in the same stand as the stepper motor gear, and connects to a LakeShore model 218 temperature monitor which reads out all six RTDs. The stepper motor controller and LakeShore are controlled and read out by a purpose built LabVIEW application ("Application"). The Application has a graphical interface to display both the temperature measurements and motor drive conditions and writes data files which are then accessible by network for offline analysis.

The RTDs are platinum, type K 100 Ohm and were not calibrated, either from the manufacturer or by us before their use. However, the RTD devices were immersed in liquid nitrogen upon their arrival and found to be accurate to within 0.5 Kelvin. For the data presented here, the temperature offsets at LAr temperatures were adjusted in software to overlap for all three RTDs on a single Spooler. It should be noted that the LAr in the LAPD tank is not at thermal equilibrium since the vapor is continually being removed and condensed in an external condenser, then admixed with LAr drawn directly from the tank and then sent through purification filters before being returned to the tank. This evaporation of LAr from the surface is seen visually by a surface turbulence, and detected by the Spooler RTDs as a temperature drop both from the bulk liquid below the surface, and the vapor above in the ullage.

The RTD circuit board is normally parked at the top limit switch. During a typical run, the Application moves the RTD circuit board twenty equal steps downward, and then reverses direction and moves the Spooler up using the same number and size of the steps. At each step motion, the Application pauses for a predetermined wait-after-move time. After this pause, the three RTDs of a single Spooler are scanned sequentially. In order to improve the precision of the temperature measurement, the Lakeshore was setup to average (in an exponential window) up to 64 points per RTD readout. After this scan, the application waits another period of time. This wait time was chosen to be long enough to ensure the exponential averaging window has been filled with new data points. Then the three RTDs are scanned again. This is repeated one more time so that at any vertical position, each RTD is measured three times.

The motivation for the three measurements of each RTD at every vertical location is that it is useful to see if the temperature is constant over this period, both to understand the inherent precision of the measurement, but also to see that the RTDs are in actual thermal equilibrium with the argon. In the case of determining the measurement precision, one expects a random scatter of temperature vs the measurement order, while in the case of non-thermal equilibrium, the variation of RTD temperature vs. the measurement order monotonically increases or decreases. In the case that the RTD is in the liquid, the RTD appears to quickly come to thermal equilibrium even for relatively short wait periods, since the thermal heat transfer with liquid is very good. However in the gas, the thermal heat transfer is much slower. This is exacerbated by the circuit board material that the RTD is in close proximity with. In order to make precise

Figure 15. RTD Spooler inside LAPD

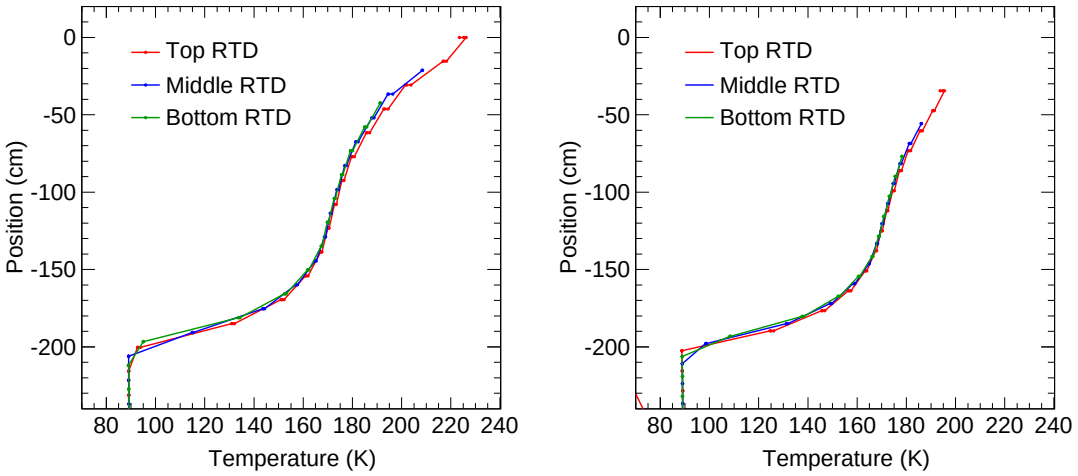

Figure 16. The tank temperature as measured by the three central (left) and the three peripheral (right) RTDs..

measurements in the gas, the wait-after-move time needed to be 30 minutes, particularly where the temperature gradient was high. In general the wait-after-move time was setup to be much less than this, since our main concern was with any temperature gradient in the liquid. Waiting long periods of time introduces other issues with variations of the cryostat total internal pressure (barometric and internal gauge pressure). At the level of 5-10mK, these variations impact the temperature. Due to thermal lags, it is difficult to accurately correct for pressure variations even though we knew the total pressure during the time of the run.

Figure 16 shows a scan of the cryostat taken after the first fill of LAr level for the central and peripheral RTD spoolers. Of primary note is the very sharp temperature gradient (80K/50cm) in the ullage just above the liquid surface. The RTD positions are corrected for the height from the top limit switch of RTD Spooler 1 (0 cm, which is almost the underside of the top center of the tank). RTDs 1-3 were on the Spooler#1, while 5-7 were on the Spooler #2. The top of the LAr surface was 2.9m (115") below this point at the date of this particular run. The data shown were taken only from the downward direction of the total run, to avoid the thermal lag one sees when the circuit board is moving out of the liquid (the wait-after-move time was 5 minutes in this case).

Figure 17 shows a relatively quick scan (downward direction too) of Spooler #2 with the Cryostat full and the wait-after-move time of 3 minutes. It should be noted that the lowest RTD of this Spooler is located just slightly above the LAr level, even with the circuit board at the top of the limit switch. However the lower tip of the circuit board is just dipping or very near the liquid surface. As a result, we think, that the heat conduction in the circuit board, this lower RTD temperature is biased lower than it would actually be if the circuit board tip were not there. As the circuit board is lowered into the LAr, one can see the temperature dip (0.4K) below the temperature of the bulk liquid. This is just the evaporative cooling of the surface layer of the LAr. Once the RTDs penetrate this surface layer, the temperature recovers to almost a constant value. It temperature scale should be noted here. The slight change of temperature with depth is less than 25mK over 2m. At the bottom of the scan there is another dip of 30mK. The returning purified LAr is introduced at the bottom of the tank and may be

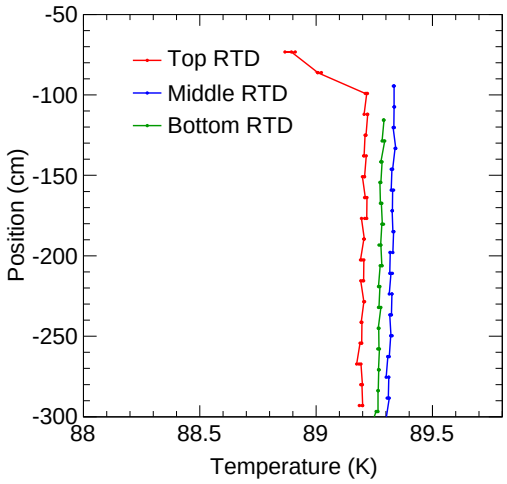

Figure 17. The temperature as measured by the three central RTDs when submerged in liquid argon. This figure illustrates the precison with which the temperature is measured.

the cause of this slight dip. Looking at the spread in measurements of any one RTD at a fixed position in the liquid, the peak-to-peak spread is 10mK, implying the relative precision of a single measurement is on the order of a few mK. There is a nominal agreement between our measurements and FEA calculations ([**?**]). This gives rise to the hope that we can use the FEA with some confidence in actual detector configurations.

4.3.1. Future work

Can omit this entirely or move to the discussion. There are a few improvements we are planning to make with the RTD Spooler System. As mentioned, we plan to make an absolute calibration of the RTDs on the circuit board in order to make an absolute temperature measurement. This precision of this calibration is not expected to be as good as our relative precision. We plan on improving the mechanical issues by changing the pcb attachment to the chain so that the pcb hangs vertically. Currently it isn't clear what the pcb angle to the vertical becomes when the pcb enters the the LAr. Another modification is to position the RTDs further away from the pcb surface. This should improve the time for the RTD to come to equilibrium with the medium after each move.

5. Results from Operation Modes

The LAPD was operated in two separate run periods. In each period, the tank was operated in three phases; a gaseous argon purge, gaseous argon recirculation, and liquid recirculation. The first Run Period was September 2011 to April 2012. Each of the three phases of operation were performed to test the devices and filters. For this period, the tank was only filled 1/3 full to confirm the feasibility of measuring the liquid argon purity Need a little more motivation and explanation of relevant events here. The second period was from December 2012 through October 2013. For this period, we performed a single argon purge at the beginning of the period, followed by a single phase of gaseous argon recirculation. The tank was then filled with liquid argon and measurements of the liquid argon purity were performed under various operating conditions.

This section describes the results for this run period, and when applicapble, measurements are compared to those obtained in the first run period.

5.1. Gaseous Argon Purge

A gaseous argon purge was peformed at the beginning of each run period. In this phase of operation, gaseous argon is pumped from the bottom of the tank displacing the ambient air which exits out the room temperature feedthroughs at the top of the tank. This mimicks an argon "piston" in the sense that the higher density gaseous argon engenders a boundary between it and the ambient air, which moves vertically upwards. For the first time interval, two sets of sampling gas capillaries were installed, leading to oxygen sensors, to measure the oxygen concentration and follow the rise of the argon gas as it displaces the lighter room air. The central set was placed on the tank axis, the peripheral set was 44 inches radially out. The sampling tube inlets were spaced 30 inches apart, spanning the height of the tank.

The purpose of these measurements was to understand the average gas purity and gain enough information for comparion to FEA flow models to validate or improve those models. The spatial and temporal concentration measurements provides information about the degree of diffusion and mixing during purges. Each purge lasted approximately 8 volume exchanges (∼24 hours) and corresponds to a 3.8 ft/hour piston rise rate and 2.9 (3.4) hours per volume exchange for the first (second) run periods, respectively. The gaseous argon flow rate was constant throughout each purge. Figure 18 shows the fraction of ambient air retained with respect to the measured oxygen levels during the gaseous argon purge in Run Period 1 for the seven capillary tubes installed in the central region of the tank and the six capillary tubes installed in the peripheral region of the tank. Insert a couple of tables for the positions? The front of gaseous argon is clearly present as indicated by the successive reduction of air seen by each capillary tube as a function of time. After 2.75 volume exchanges, corresponding to 8 hours, the oxygen level was reduced from 21% to xx.

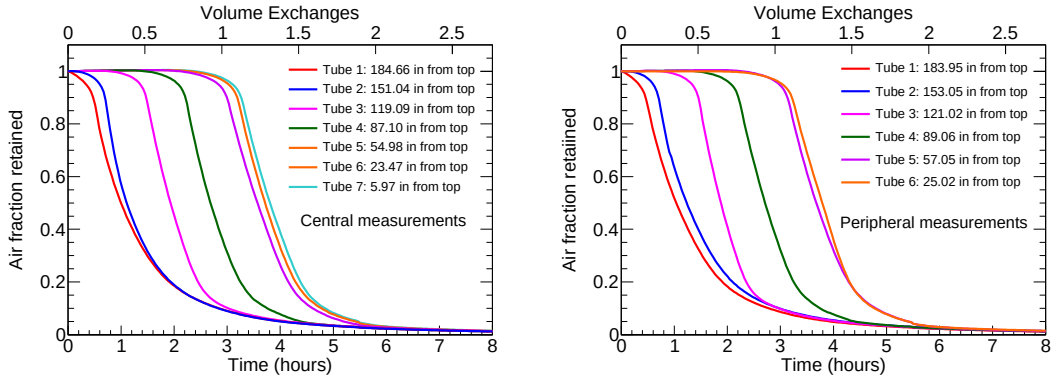

Figure 18. Oxygen concentrations for the a) central and b) peripheral gas sampling capillaries taken at several heights with respect to the tank bottom obtained during the initial gaseous argon purge for Run Period 1.

At the end of the purge, the capillaries were removed. This procedure lasted 15 minutes, during which time argon gas flowed into the tank at 5-6 SCFM. During the extraction, the

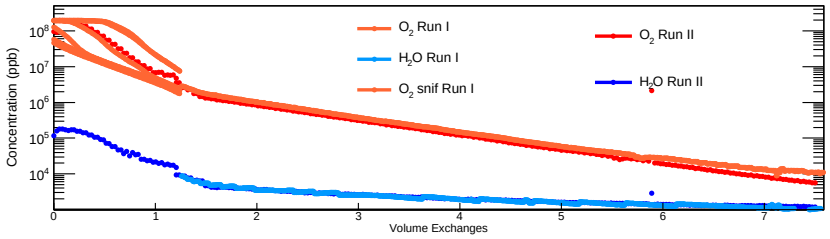

Figure 19. Water and oxygen concentrations in the LAPD during the two gaseous argon purges from Run Period 1 and Run Period 2. Probably does not look good in black and white. Also two noise points?

water, oxygen, and nitrogen monitors were switched to argon gas utility as a precaution because the bellows pump drawing gas from the tank could pull a vacuum on the tank if the argon flow into the tank stopped. After these devices were switched back to measuring the tank gas, an increase of about 0.2 ppm O_2 and 0.4 ppm N_2 was observed. With the capillaries removed, the makeup gas flow dropped from 0.35 SCFM to 0.15 SCFM. At the end of the purge, 7158 ft^3 had passed through the tank, corresponding to 8.2 volume exchanges. The oxygen level was reduced to 5.2 ppm, the water concentration was reduced to 996 ppb, and the nitrogen concentration was reduced to 13.4 ppm. Figure 19 shows the concentrations of water and oxygen during the two gaseous argon purges along with the results from the capillary tube oxygen measurements. In both run periods the water concentration was reduced to approximately 1 ppm. The oxygen concentrations were reduced to 10 and 7 ppm for Run Periods One and Two, respectively. Throughout both purges, the nitrogen concentration remained nominally stable at 18 ppm. The argon purges for both run periods delivered similar results.

5.2. Gas Recirculation

After the removal of the ambient air from the argon purge, argon gas was pumped through the molecular sieve and oxygen filter at a rate of a volume exchange every 3.4 hours, then returned to the tank. The gas recirculation for Run Period Two ran for about 77 volume exchanges (about 1 week). Figure 20 shows the oxygen and water concentrations, measured by the HaloTrace and Nanotrace, respectively, for the gas recirculation phase. At the end of this phase, the oxygen concentration was reduced to approximately 20 ppb. The water concentration was stable at 667 ppb. This indicates that the water outgasses from where? and forever. Note also that the outgassing rate eventually matches the filtration rate. The nitrogen was reduced to 13.7 ppm.

Figure 21 shows the water and oxygen concentrations measured in the gas in the tank vapor space. Need to describe these plots, in terms of the switching the devices from measuring in the liquid to measuring in the gas. This is for events in February and March

Figure 22 shows the water and oxygen concentrations measured in the gas in the tank vapor space. Need to describe these plots, in terms of the switching the devices from measuring in the liquid to measuring in the gas. This is for events in August and September.

5.3. Liquid Argon Filling

For Run Period 1, the tank was only filled to 1/3 capacity, which ended untimely due to a power outage or some other excuse. For Run Period 2, the tank was filled with LAr from the D0 calorimeters at Fermilab in four trailer loads. The duration of each tank fill varied from 4 to

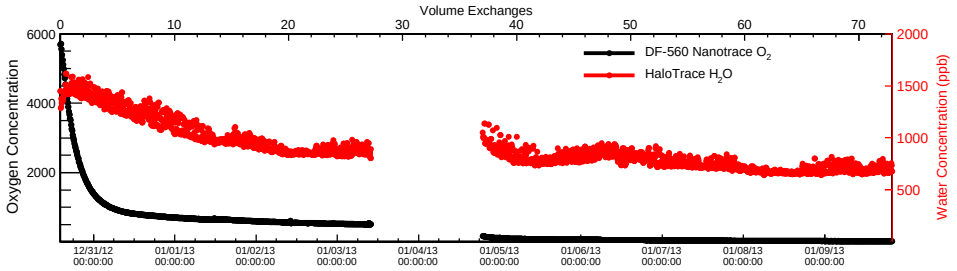

Figure 20. The water and oxygen concentrations in the tank gas during the gas recirculation phase of Run Period 2. Should be log scale? Also need explanation for the gap.

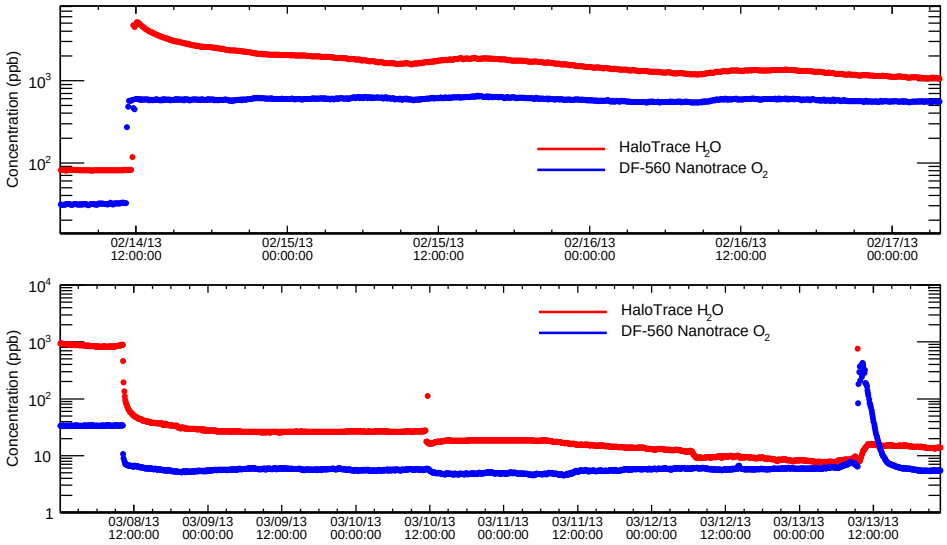

Figure 21. The water and oxygen concentrations in the gas of the vapor space at the top of the tank with the tank totally filled. Measurements were taken in the tank vapor at the 29 inch feed through and then on February 14, 2013 in the tank vapor at the top of the TPC feed through.

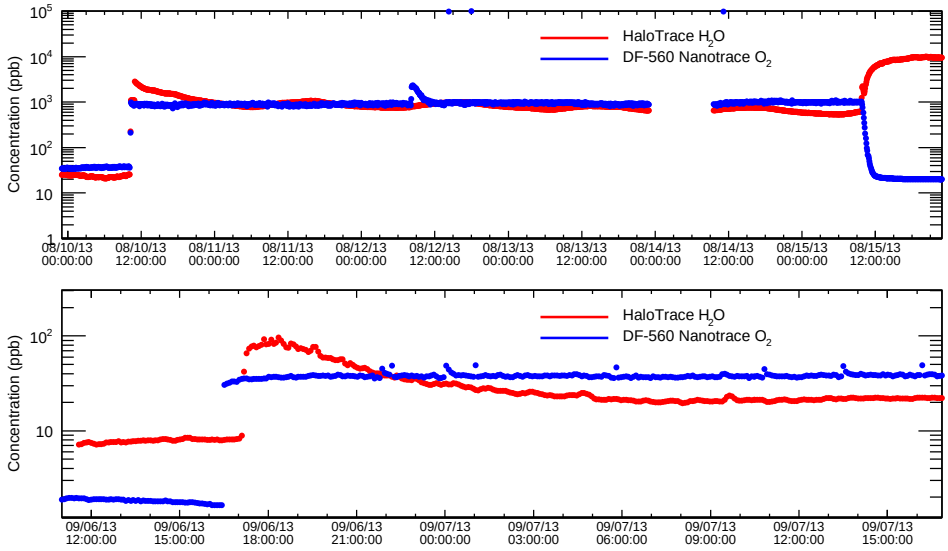

Figure 22. The water and oxygen concentrations in the gas of the vapor space at the top of the tank with the tank totally filled.

6 hours. Table 2 presents the LAr trailer contaminant concentrations along with details of each successive fill for Run Period 2. The four trailers were delivered over a period of two weeks in January, 2013. The total volume of LAr placed in the tank was 5630 gallons, corresponding to 29.7 tonnes.

5.4. Liquid Argon Recirculation

After the tank was full, the liquid recirculation pump was started at a rate of 9.4 GPM. Filtration proceeded by routing liquid argon through the two filters. We had several opportunities to determine the performance of the filters and their capability to reduce the impurities, at various times throughout operation. Figure 23 shows the water and oxygen concentrations in the tank liquid as measured by the HaloTrace and Nanotrace as a function of time, for three select intervals immediately preceding purity monitor operation. The measured oxygen concentration

	O_2 (ppb)	H_2O (ppb)	N_2 (ppm)	LAr height (inches)	GPF	Rate (GPM)	Net gallons
Trailer 1	202	99	10	27	1325	$\approx$ 500	1325
Trailer 2	200	225	9	58	2832	587	1507
Trailer 3	400	180	9	87	4259	520	1427
Trailer 4	197	66	10	115	5630	400-525	1371

Table 2
Concentrations of oxygen, water, and nitrogen measured in each trailer before introduction into LAPD. The LAr height is measured in inches from the bottom of the tank corresponding to the number of gallons delivered to the tank in each fill (GPF). Also shown is the rate in gallons per minute (GPM).

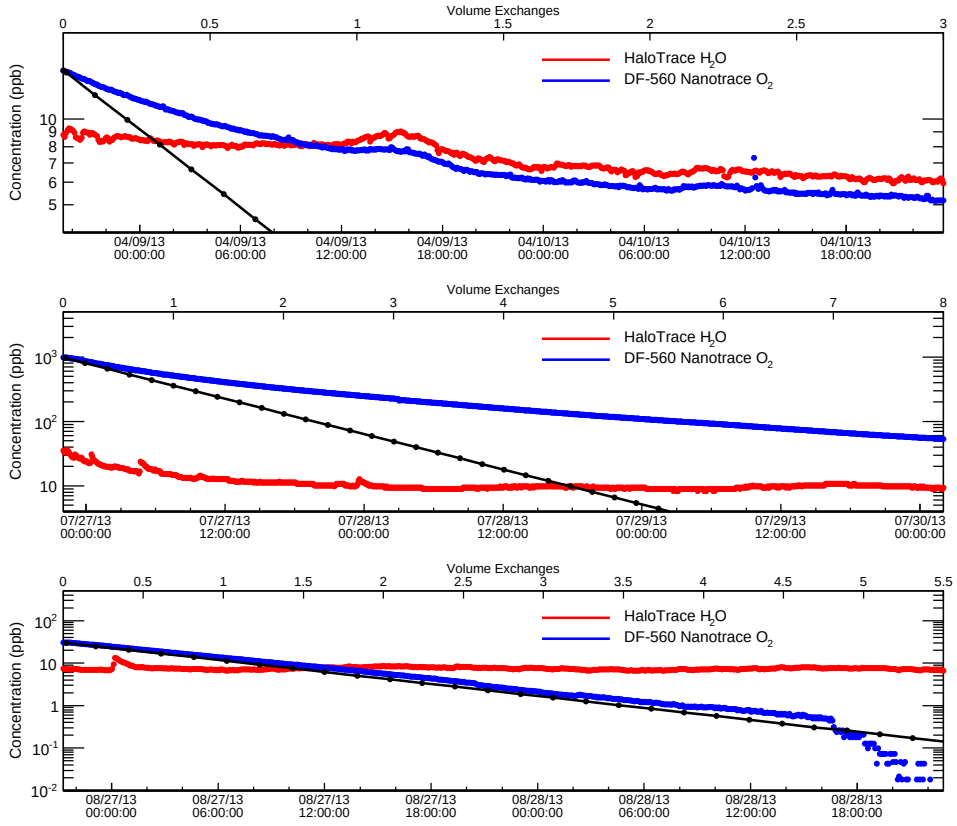

Figure 23. The water and oxygen concentrations in the tank liquid for three time intervals before purity monitor operation. The measured oxygen concentration (blue line) is compared to a simulation assuming perfect mixing (black line).

was compared to simulation assuming perfect mixing in the tank (Need explanation for "perfect mixing"). The figure shows that in the first two time intervals, perfect mixing was not achieved. This suggests that what?. However, in the last time interval, perfect mixing was nearly achieved.

Figure 24 shows the water and oxygen concentrations measured in the tank vapor space with the tank totally filled with LAr, along with the temperature in the LAPD hall. The temperature and the water concentration in the tank vapor space are closely correlated. Need to finish this story.

After several liquid volume exchanges, the contamination was sufficiently low to begin operation of the four purity monitors inside the tank and the inline purity monitor upstream from the filters. The signal attenuation is defined as $1 - Q_A/Q_C$, where Q_A and Q_C are the anode and cathode peak pulse heights, respectively. The pump speed, and thus the volume exchange rate were changed over several time intervals to determine if this affected the lifetime. Figure 25 shows the attenuation and pump speed over the full range of running. I think we should break this up, probably at least into the regions where we achieved a good cleanup . Needs more discussion.

Figure 26 shows a period of time when the LAPD experienced a pump failure. This figure

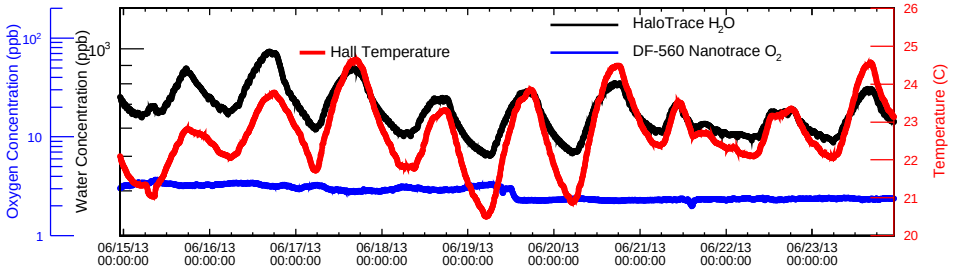

Figure 24. The water and oxygen concentrations measured in the tank vapor space with the tank totally filled with LAr. Also shown is the temperature in the LAPD hall for the same time period.

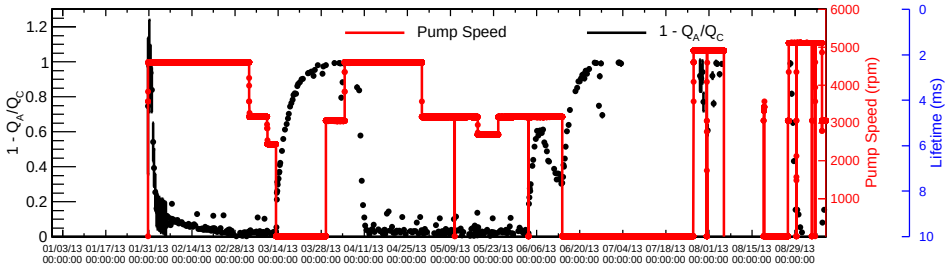

Figure 25. The attenuation (1 - Q_A/Q_C) for recirculated liquid argon over all LAPD running. The attenuation is correlated with electron lifetime, also shown on the right-hand scale. NOTE: This is old data that needs the few percent correction. Also shown is the pump speed.

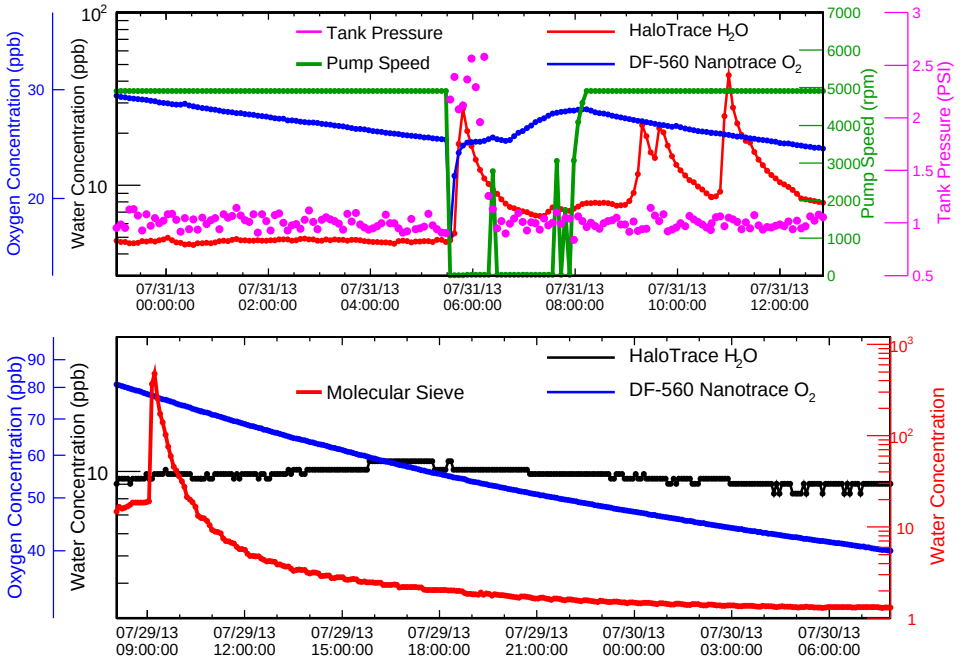

Figure 26. Top: The tank pressure, pump speed, and the oxygen and water concentrations in the tank liquid during an event when the pump was briefly turned off. Bottom: The oxygen and water concentrations measured in the tank liquid compared to the water concentration measured in the molecular sieve over the same time period. Tank cleanup drastically falls behind cleanup in the molecular sieve, etc.

also shows the water concentration in the molecular sieve. Needs more discussion if we want to include this.

6. Discussion and Conclusion

This needs some work. The primary goal of the Liquid Argon Purity Demonstrator (LAPD) has been achieved. The required level of purity can be achieved in a large volume of liquid argon without first evacuating the vessel containing the liquid and LArTPC. This test is motivated by the desire to obviate costs associated with the construction of an evacuable cryostat for future multi-kiloton detectors.

In addition to showing that evacuation is not necessary for achieving long electron lifetimes, we studied temperature gradients, liquid argon volume exchanges, filter capacity, and the effect of other materials. Discuss each of these. The results demonstrated that the technique works in the presence of material and nominal electron drift lifetimes were recovered after X minutes.

Indications from the MTS suggest the water concentration increases as the sample temperature increases, and the electron lifetime decreases. This demonstrates two major findings from the MTS. First, there is a direct relationship between electron lifetime and water concentration. Second, the water concentration does not change when materials are submerged in the liquid, but it does increase when materials are in the vapor space. Attention was given to how one would scale the system for kiloton scale masses of liquid argon and the potential scaling of the

cost for such large systems. Initial estimates indicate that the cost of larger systems does not scale linearly with volume.

Acknowledgments

We thank the staff at FNAL for their technical assistance in running the LAPD experiment. We acknowledge support by the Grants Agencies of the DOE.

REFERENCES

1. T. Akiri *et al.* (LBNE Collaboration), arXiv:1110.6249 [hep-ex].
2. S. Amerio *et al.* (ICARUS Collaboration), Nucl. Instrum. Meth. A **527**, 329 (2004).
3. C. Rubbia, *et al.* (ICARUS Collaboration), Journal of Instrumentation, **6** P07011 (2011).
4. R. Andrews, W. Jaskierny, H. Jostlein, C. Kendziora, S. Pordes and T. Tope, Nucl. Instrum. Meth. A **608**, 251 (2009).
5. W. Jaskierny, H. Jostlein, S. H. Pordes, P. A. Rapidis and T. Tope, FERMILAB-TM-2384-E.
6. C. Anderson, *et al.* (ArgoNeuT Collaboration), Journal of Instrumentation, **7**, P10019 (2012).
7. A. Ereditato, *et al.*, Journal of Instrumentation, **8**, P7002 (2013).
8. B. Rebel, M. Adamowski, W. Jaskierny, H. Jostlein, C. Kendziora, R. Plunkett, S. Pordes and R. Schmitt, T. Tope and T. Yang, J. Phys. Conf. Ser. **308**, 012023 (2011).
9. G. Carugno, B. Dainese, F. Pietropaolo and F. Ptohos, Nucl. Instrum. Meth. A **292**, 580 (1990).
10. O. Bunneman, B. Cranshaw and J.A. Harvey, Can J. Res. **27**, 191 (1949)
11. E. Voirin, LAPD Cryostat Interior temperatures-RTD measurements and CFD models of Liquid and Gas Temperatures, LARTPC-doc-635-v4, 5/13/2013